Laser and Particle Beams (2002), *20*, 589–593. Printed in the USA.

DOI: 10.1017/S0263034602204176

Bunching dynamics and transport window of intense ion beams in final beam buncher

TAKASHI KIKUCHI, MITSUO NAKAJIMA, AND KAZUHIKO HORIOKA
Department of Energy Sciences, Tokyo Institute of Technology, Nagatsuta 4259, Midori-ku, Yokohama, 226-8502, Japan

(RECEIVED 27 May 2002; ACCEPTED 19 June 2002)

Abstract

A longitudinal compression is indispensable in a final stage of the heavy ion driver system using a particle accelerator. For the beam compression, an induction buncher applies the bunching voltage so as to make a considerable velocity tilt between the head and the tail of the beam bunch. However, the velocity tilt induces mismatch oscillation of the beam envelope due to the nonconformity between the beam particle velocity and the confinement force of the lens system. At the first step of design works for the beam transport line, the initial phase advance is decided to avoid resonance lines on the tune diagram. However, as the phase advance changes in the buncher by the velocity tilt, the beam bunch reenters in the resonance condition under certain circumstances. The transport region for avoiding the resonance condition is discussed on a phase diagram, as a function of the phase advance and the velocity tilt.

Keywords: Beam bunching; Heavy ion fusion; Induction buncher; Intense ion beams; Particle-core model

An intense heavy ion beam, which has extreme parameters of ~10 GeV particle energy, total beam current of ~100 kA, and ~10-ns pulse duration, is required for a suitable implosion of a fuel pellet in heavy ion inertial fusion (HIF; Barnard *et al.*, 1993, 1998; Hofmann, 2000). A longitudinal compression is indispensable in the final stage of the driver system. In the final stage, the beam pulse duration must be shortened from ~100 ns to ~10 ns for the effective pellet implosion (de Hoon *et al.*, 2001; Lee & Barnard, 2001; Qin *et al.*, 2001).

For the beam compression, an induction buncher applies the bunching voltage so as to make a considerable velocity tilt between the head and the tail of the beam bunch. For the inductive beam modulation, bipolar bunching waveforms are desirable, because the core of the induction modules needs reset pulses (Watanabe *et al*., 2002). The induction buncher unit consists of acceleration gaps and a focusing-off (drift)-defocusing-off (drift) (FODO) configuration quadrupole lattice for the transverse beam confinement (Reiser, 1994; Davidson & Qin, 2001). The transverse confinement force and the lattice structures are carefully designed for the beam envelope matching.

Address correspondence and reprint requests to: Takashi Kikuchi, Department of Energy Sciences, Tokyo Institute of Technology, Nagatsuta 4259, Midori-ku, Yokohama, 226-8502, Japan. E-mail: tkikuchi@es.titech.ac.jp

However, the large head-to-tail velocity tilt may cause mismatch oscillation of the beam envelope due to the nonconformity between the beam particle velocity and the magnetic confinement force (Kim *et al.*, 1986). At the first step of design work for the beam transport line, the initial phase advance is decided to avoid resonance lines on the tune diagram. However, as the phase advance changes by the velocity tilt and the perveance increases during the beam bunching, the beam bunch reenters into resonance conditions under certain circumstances. The induced transverse mismatch and the resonance effect may cause chaotic behavior of the beam particle, a halo formation and an emittance growth of the beam, during the compression process. Consequently, the unfavorable behavior should be avoided from the viewpoint of the high-quality beam transport.

In this study, we estimate a transport window of the bunching beam with large head-to-tail velocity tilt. The transport window is defined by a region for avoiding the resonance conditions, and is illustrated in a diagram as a function of the phase advance and the velocity tilt. We consider the estimation of transport window using a particle-core model (PCM; Lagniel, 1994; Qian *et al.*, 1995; Ikegami, 1999).

We use beam envelope equations and PCM for the analyses of the bunching beam behavior. The transverse envelope equations are based on the well-known assumption of Kapchinskij–Vladimirskij (KV) distribution beams (Kapchinskij & Vladimirskij, 1959). The transverse enve-

lopes, X and Y along the transport direction s, are calculated by

$$\frac{d^2X}{ds^2} = -k_t hX + \frac{2K}{X+Y} + \frac{\varepsilon_t^2}{X^3}, \tag{1a}$$

$$\frac{d^2Y}{ds^2} = -k_t hY + \frac{2K}{X+Y} + \frac{\varepsilon_t^2}{Y^3}, \tag{1b}$$

where k_t is the transverse confinement force, h is an alternating step function, K is the transverse perveance, and ε_t is the transverse emittance. The perveance K is defined by

$$K = \frac{q^2 N}{4\pi\varepsilon_0 mc^2\beta^2\gamma^3}\frac{1}{Z}, \tag{2}$$

where q is the charge state of the beam ion, e is elementary charge, N is the ion number of the beam bunch, ε_0 is the permittivity of free space, m is the mass of the beam ion, c is the speed of light, Z is the longitudinal beam envelope, β is the velocity divided by c, and γ is the relativistic factor at the center of longitudinal beam position.

As Figure 1 shows, the function h is given by

$$h(s) = h(s+S), \tag{3}$$

in the case of FODO lattice with the one-period length S. The confinement force k is defined as

$$k = \frac{qB}{mc\beta\gamma a_q}, \tag{4}$$

where B is the magnetic force of the FODO lattice and a_q is the bore radius of the FODO quadrupole magnet.

Assuming the parabolic line charge density λ for the longitudinal direction as shown in Figure 2, the longitudinal beam behavior can be described as

$$\frac{d^2Z}{ds^2} = -k_z h' + \frac{K_L}{Z^2}, \tag{5}$$

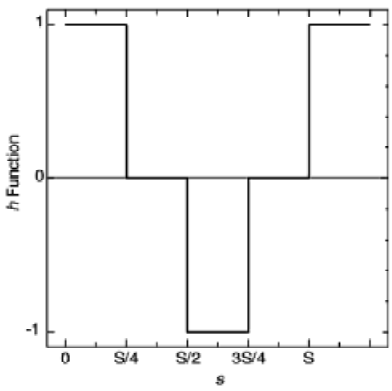

Fig. 1. The h function FODO lattice.

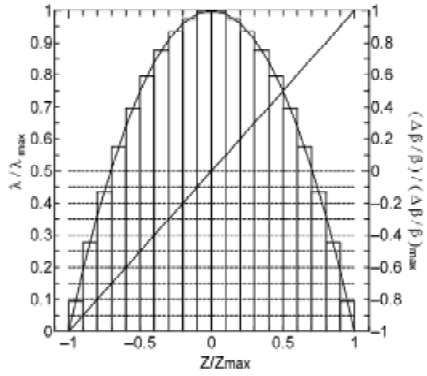

Fig. 2. Assumed parabolic line charge density and linear velocity tile distributions along the longitudinal direction.

where k_z is the applied linear force for the beam bunching, h' is given as

$$h'(s) = \begin{cases} 1, & \text{if } h = 0 \\ 0, & \text{otherwise} \end{cases}, \tag{6}$$

and K_L is the longitudinal perveance, which is defined by

$$K_L = \frac{3}{2}\frac{gNr_c}{\beta^2\gamma^5}, \tag{7}$$

g is the geometry factor and r_c is the classical particle radius.

By numerically solving the above equations simultaneously, we can calculate the beam envelope dynamics. The typical longitudinal beam dynamics are shown in Figure 3, and the transverse envelopes at the beam center are shown in Figure 4. As Figure 3 shows, while the bunch length is compressed to the required value, the head-to-tail velocity tilt is varied up to 5%. During the beam compression process, the beam radius expands along the transport distance as shown in Figure 4.

Since k and K depend on the velocity of the beam, the transverse envelopes described by Eq. (1a) and Eq. (1b) are

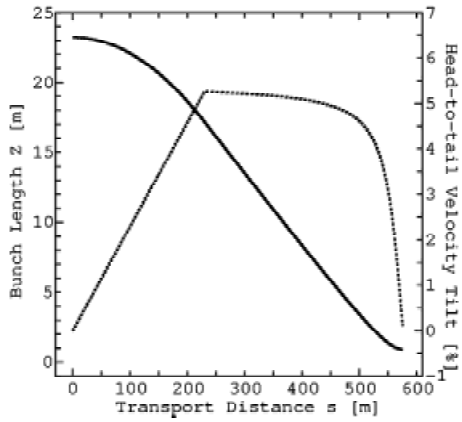

Fig. 3. Bunch length (solid line) and velocity tile (dotted line) as a function of transport distance.

https://doi.org/10.1017/S0263034602204176 Published online by Cambridge University Press

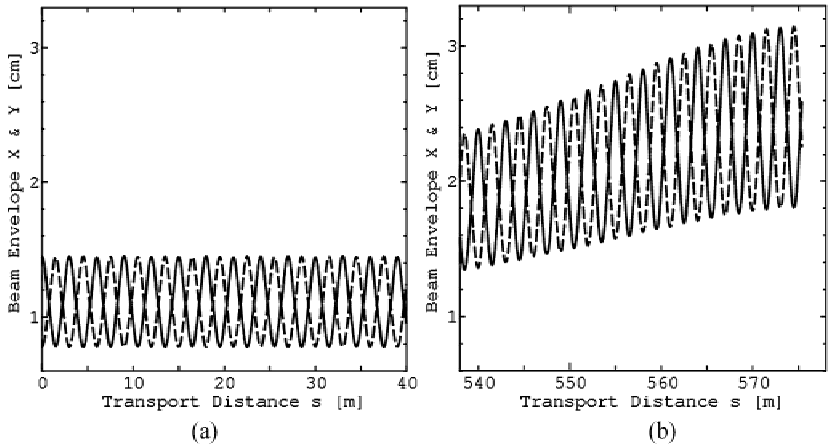

Fig. 4. Transverse envelope X (solid) and Y (dashed) variations at the beam center due to the longitudinal beam compression at the start point (a) and at the final region (b).

modulated by the applied head-to-tail velocity tilt $\Delta\beta/\beta$. The velocity tilt is defined as

$$\frac{\Delta\beta}{\beta} = \frac{\beta_t - \beta_h}{\beta_c}, \tag{8}$$

where β_h, β_t, and β_c denote the values at the head, in the tail part, and in the center of the beam, respectively.

As is well known, the phase advances of 90°, 72°, 60°, and 51.4° (= 360/n for integer n) are typical values of the resonance conditions. If the betatron tune of the beam enters the forbidden values, the beam becomes resonantly unstable. Even if the initial phase advance (without space charge) σ_0 is decided far from the resonance line, the bunching beams with large compression ratio inevitably have large velocity tilts and the phase advance (with space charge) σ is strongly depressed by the space charge effect. Thus the phase advance is considerably modulated in the final buncher.

The relation between the FODO lattice parameters and σ_0 is given as

$$\cos\sigma_0 = \cos\theta\cosh\theta + \frac{L}{\ell}\theta(\cos\theta\sinh\theta - \sin\theta\cosh\theta)$$
$$-\frac{1}{2}\left(\frac{L}{\ell}\right)^2\theta^2\sin\theta\sinh\theta \tag{9}$$

and

$$k = \left(\frac{\theta}{\ell}\right)^2, \tag{10}$$

where ℓ is the length of the quadrupole lens space (F or D in FODO), L is the length of the drift space (O in FODO), and θ is the focusing strength of the magnetic quadrupole lens (Reiser, 1994). The average beam radius $\bar{a}$ is calculated approximately as (Stewart & Hubbard, 1992):

$$\bar{a}^2 = \frac{2\varepsilon_t(\ell + L)}{\sin\sigma}. \tag{11}$$

The normalized transverse emittance $\varepsilon_n = \beta\gamma\varepsilon_t$ is assumed to be 13 mm-mrad. Using $\bar{a}$, the relation between σ_0 and σ is given approximately from

$$\cos\sigma - \cos\sigma_0 = 2K\left(\frac{\ell + L}{\bar{a}}\right)^2. \tag{12}$$

Using Eqs. (9)–(12), we can estimate the relation between the phase advance with and without space charge. In addition, we calculate the modulated phase advances with the velocity tilt, from Eqs. (2), (4), and (8).

Based on the discussion above, we can analytically draw the modulation of phase advance as a function of $\Delta\beta/\beta$ and K. Figure 5 shows an example around $\sigma_0 = 90°, 72°, 60°$. In Figure 5, the solid lines give the upper limit for avoiding the resonance condition, and the dotted lines indicate the lower limit for avoiding the resonance condition at the beam tail

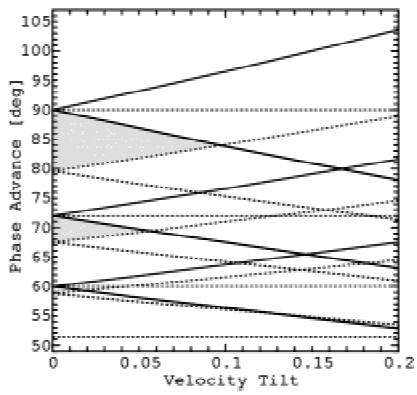

Fig. 5. Transport window for avoiding the resonance lines of 90°, 72°, 60°, and 51.4°.

https://doi.org/10.1017/S0263034602204176 Published online by Cambridge University Press

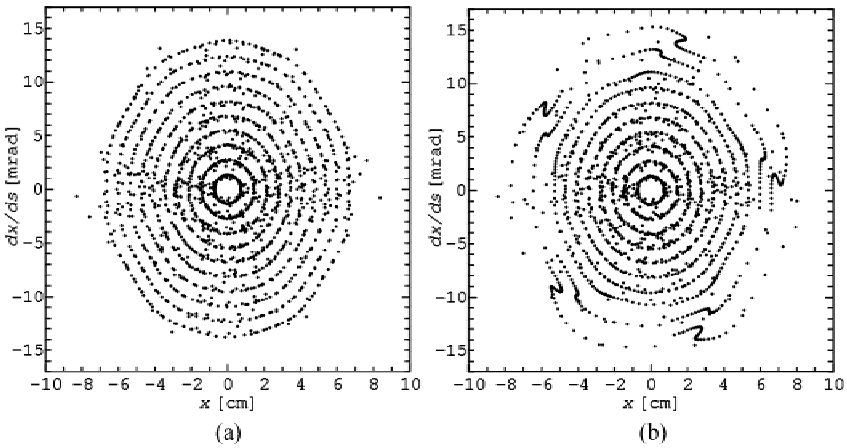

Fig. 6. Poincaré plots of test particles (a) at the beam center and (b) at $Z/3$ along the longitudinal beam direction.

and head. In this study, we assumed the beam parameters of the final stage in HIF driver (Barnard *et al.*, 1993). Since the stable condition of the beam transport should be satisfied for all of the particles from the head to the tail of the beam bunch, the overlap region of the head and tail lines for the beam shows the transport window in case of bipolar bunching waveforms.

If the beam parameter is outside of the transport window, unstable behavior of the specific beam particles is predicted. For that reason, we investigate the beam particle behaviors by PCM. In the PCM simulation, we assume the longitudinal perveance and the applied velocity tilt as the distribution of Figure 2. For the calculation of the beam core, we use the KV envelope equations (1)–(8). The test particle equations of X-direction are written by

$$\frac{d^2x}{ds^2} = -k_t hx + \begin{cases} \dfrac{2K}{X(X+Y)}\,x, & |x| \le X \\ \dfrac{\mathrm{sgn}(x)\cdot 2K}{|x| + \sqrt{x^2 + Y^2 - X^2}}, & |x| > X \end{cases}, \qquad (13)$$

where x is the test particle position (Lagniel, 1994; Ikegami, 1999). The test particles are placed in and out of the beam core at the initial condition.

Figure 6 shows the Poincaré surface plots in the case of $\sigma_0 = 72°$ during the longitudinal beam compression. Since Figure 6a shows the Poincaré plot at the center of the beam bunch, the head-to-tail velocity tilt is not applied. On the other hand, Figure 6b shows the Poincaré plot at $Z/3$, and the resonance effect of $\sigma_0 = 72°$ appeared around the beam core as predicted by the transport window of Figure 5.

In summary, the transport region, which can be avoided from the resonance lines, was estimated on the phase diagram. The transport window was illustrated in the diagram as a function of the phase advance and the velocity tilt. Using PCM calculations, we demonstrated the beam particle behavior. As a result, it is found that the criterion can practically predict the transportability of the bunching beam.

We did not consider self-consistently the beam dynamics during the longitudinal compression in this study. A self-consistent analysis of the transport of the bunching beam is also now in progress. However, we think that the simplified criterion is useful as the first step evaluation of the transport line design for the final buncher in HIF, and allows us to have an insight in the interpretation of the more detailed simulation results.

REFERENCES

Barnard, J.J., Bangerter, R.O., Faltens, A., Fessenden, T.J., Friedman, A., Lee, E.P., Logan, B.G., Lund, S.M., Meier, W., Sharp, W.M. & Yu, S.S. (1998). Induction accelerator architectures for heavy-ion fusion. *Nucl. Instrum. Methods Phys. Res. A* **415**, 218.

Barnard, J.J., Deadrick, F., Friedman, A., Grote, D.P., Griffith, L.V., Kirbie, H.C., Neil, V.K., Newton, M.A., Paul, A.C., Sharp, W.M., Shay, H.D., Bangerter, R.O., Faltens, A., Fong, C.G., Judd, D.L., Lee, E.P., Reginato, L.L., Yu, S.S. & Godlove, T.F. (1993). Recirculating induction accelerator as driver for heavy ion fusion. *Phys. Fluids B* **5**, 2698.

Davidson, R.C. & Qin, H. (2001). *Physics of Intense Charged Particle Beams in High Energy Accelerators*. Singapore: World Scientific.

de Hoon, M.J.L., Lee, E.P. & Barnard, J.J. (2001). Drift compression of space charge dominated beams. *Proc. 2001 Particle Accelerator Conf., Chicago*. Vol. 1, p. 729. Piscataway, NJ: IEEE.

Hofmann, I. (2000). Recent developments in heavy ion driver studies at GSI. *Proc. First Intl. Conf. Inertial Fusion Sciences and Applications* (IFSA 99), Bordeaux. p. 12. Paris: Elsevier.

Ikegami, M. (1999). Particle-core analysis of mistatched beams in a periodic focusing channel. *Phys. Rev. E* **59**, 2330.

Kapchinskij, I.M. & Vladimirskij, V.V. (1959). Limitations of proton beam current in a strong focusing linear accelerator

https://doi.org/10.1017/S0263034602204176 Published online by Cambridge University Press

associated with the beam space charge. *Proc. Int. Conf. High Energy Accelerators and Instrumentation*. p. 274. Geneva: CERN Scientific Information Service.

Kim, C.H., Judd, D.L., Laslett, L.J., Smith, L. & Warwick, A.I. (1986). Head-to-tail velocity tilt in an ion induction LINAC. AIP Conf. Proc. 152. p. 264. New York: American Institute of Physics.

Lagniel, J.-M. (1994). Chaotic behaviour and halo formation from 2-D space-charge dominated beams. *Nucl. Instrum. Methods Phys. Res. A* **345**, 405.

Lee, E.P. & Barnard, J.J. (2001). Design considerations for final pulse compression with bending for heavy ion fusion drivers. *Proc. 2001 Particle Accelerator Conf., Chicago*. Vol. 4, p. 2929. Piscataway, NJ: IEEE.

Qian, Q., Davidson, R.C. & Chen, C. (1995). Halo formation induced by density nonuniformities in intense ion beams. *Phys. Rev. E* **51**, 5216.

Qin, H., Jun, C., Davidson, R. & Heitzenroeder, P. (2001). Drift compression of space-charge-cominated bunched beams. *Proc. 2001 Particle Accelerator Conf., Chicago*. Vol. 3, p. 1761. Piscataway, NJ: IEEE.

Reiser, M. (1994). *Theory and Design of Charged Particle Beams*. New York: Wiley.

Stewart, L.D. & Hubbard, E.L. (1992). Heavy ion beam drive final drift, compression, and focusing design. *Fusion Technol.* **21**, 1594.

Watanabe, M., Nakajima, M., Shiho, M., Horioka, K., Takayama, K. & Kishiro, J. (2002). Magnetic core characteristics for high rep-rate induction modulator. *Rev. Sci. Instrum.* **73**, 1756.

https://doi.org/10.1017/S0263034602204176 Published online by Cambridge University Press